ISBN: 978-3-95450-231-8 ISSN: 2673-5490 doi: 10.18429/JACoW-IPAC2023-MOPA103

BEAM CHARACTERIZATION AND OPTIMISATION FOR AWAKE 18 MeV ELECTRON LINE

V. Bencini[1]*, S. Doebert, E. Gschwendtner, E. Granados, F.M. Velotti, L. Verra, G. Zevi Della Porta[2]
CERN, Geneva, Switzerland
[1] also at John Adams Institute for Accelerator Science, Oxford, United Kingdom
[2] also at Max Planck Institute for Physics, Munich, Germany

Abstract

After the successful conclusion of Run 1 in 2018, the AWAKE experiment is presently undergoing its second phase (Run2), which aims to demonstrate the possibility of producing high quality electron beams for high energy physics applications. Over the last year, a significant time-investment was made to study proton beam centroid modulation effects in plasma induced by a seeding electron bunch (i.e. hosing). The high beam pointing accuracy needed for the study translated into tighter constraints for the 18 MeV electrons injection line. To address the new requirements, a measurement campaign was dedicated to the characterisation and optimisation of the beam line. In the first part of this paper, we present the results of the measurements and simulations carried out for the line characterization. The second part focuses on the description of the operational tools developed to address the new beam requirements and performance.

INTRODUCTION

AWAKE Run1, concluded in 2018, demonstrated the possibility of accelerating 18 MeV electrons up to 2 GeV using the plasma wakefields induced by a 400 GeV proton beam extracted from the Super Proton Synchrotron (SPS) at CERN [1]. The aim of AWAKE Run 2 is to improve the energy reach compared to Run 1 while preserving a smaller emittance and energy spread to produce a beam suitable for high-energy physics applications [2].

Run 2a successfully demonstrated the possibility of using the beam produced in the 18 MeV witness electron line to seed the Self-Modulation of the proton bunch with reproducible phase [3]. The next step is to study the effects of relative misalignment between electron and proton bunches on the seeded self-modulation process (that is, hosing) [4]. Hosing studies set new, tighter requirements for the 18 MeV witness electron beam line.

A complete characterisation of the beam line had already been performed in 2018 [5], showing good agreement between simulations and measurements and proposing a set of operational tools to improve the set-up procedure of the beam line. However, the installation of a new scintillation screen at injection and the rise of the new beam requirements called for a new beam line characterisation and the development of further dedicated tools. This article describes the main challenges that were identified during the 2022 run and the methods and tools developed to deal with them.

Electron Line General Layout

The witness electron beam injected in the AWAKE plasma source is produced with an S-band, RF photo-cathode gun and accelerated in a traveling-wave booster linac to 18 -20 MeV [6]. The transfer line [7] described in this paper has the purpose of transporting the 18 MeV electrons to the plasma source, where they are either accelerated or used to seed the proton beam self-modulation.

The beam line is divided into four sections. A matching section after the gun, a dogleg in the vertical plane, an achromat in the horizontal plane, and the last section of the line, common to the electron and proton beams. The vertical dogleg was installed to compensate for the relative angle between the accelerating section and the proton line to allow for the coaxial propagation of the electron and proton beams in the common section. The line consists of 10 quadrupoles, 4 dipoles (2 horizontal and 2 vertical), 11 correctors (both horizontal and vertical), and 11 beam position monitors (BPM).

The transverse beam distribution can be monitored along the line thanks to 6 BTV screens. The last of these screens (BTV.EXP_VOL), installed at the end of 2021 in the expansion volume of the plasma source, allows to monitor the injected electron beam very close to the plasma entrance. A schematic of the electron line is shown in Fig. 1.

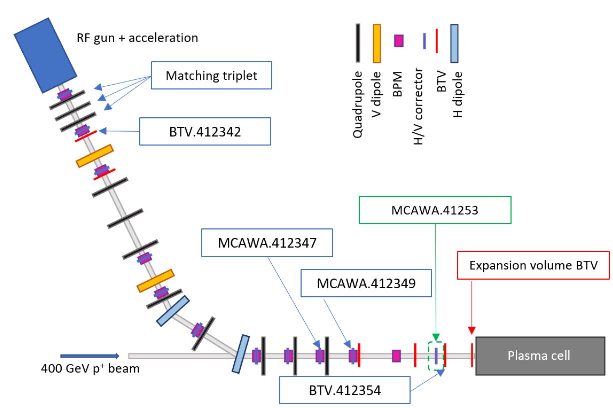

Figure 1: Layout of the 18 MeV electron injection line. Highlighted in blue, the elements already present during Run 1. In red, BTV.EXP_VOL, installed before 2022 run. In green, the new corrector installed in 2023.

* vittorio.bencini@cern.ch

Content from this work may be used under the terms of the CC BY 4.0 licence (© 2022). Any distribution of this work must maintain attribution to the author(s), title of the work, publisher, and DOI.

ISBN: 978-3-95450-231-8 ISSN: 2673-5490 doi: 10.18429/JACoW-IPAC2023-MOPA103

Content from this work may be used under the terms of the CC BY 4.0 licence (© 2022). Any distribution of this work must maintain attribution to the author(s), title of the work, publisher, and DOI.

Operational Challenges

During the measurement campaign that took place in 2022, three main operational challenges were identified, which are described in detail in the following paragraphs.

Orthogonal Steering Orthogonal steering exploits two correctors to adjust the central beam position and angle at plasma entrance. The new BTV allows to measure with high accuracy the beam position at injection, highlighting very low reproducibility of the orthogonal steering process.

Online Beam Matching The parameters of the beam generated in the photo-injector change on a daily basis, affecting the beam parameters at the end of the beam line. To minimize the set-up time of the experiment, it is critical to be able to quickly rematch the beam optics to the nominal parameters.

Beam Distribution Reconstruction Emittance measurements are preformed using a quadrupole scan [8] in a dispersion-free region at the entrance of the beam line. This method is not accurate enough to provide good agreement between tracking simulations and measurements. Therefore, a different approach had to be developed.

ORTHOGONAL STEERING

Being R_1 and R_2 the 2x2 transport matrices (in the x or y plane) between the first and the second corrector and a given observation point, the relative angular ($\Delta x'$) and position (Δx) displacement at observation point can be calculated as follows:

$$\begin{bmatrix} \Delta x \\ \Delta x' \end{bmatrix} = \begin{bmatrix} R_{1,(1,2)} & R_{2,(1,2)} \\ R_{1,(2,2)} & R_{2,(2,2)} \end{bmatrix} \begin{bmatrix} \Delta k_1 \\ \Delta k_2 \end{bmatrix} \tag{1}$$

Ideally, knowing the elements of the response matrix in Eq. (1), the kicks Δk_1 and Δk_2 needed to obtain (Δx) and ($\Delta x'$) can be calculated by inverting the matrix. During the 2022 run, measurements on the correctors MCAWA.412347 and MCAWA.412349, used for orthogonal steering, showed hysteresis. In these conditions, the response coefficients vary as a function of the previous set values. As a consequence, the response to the kicks in non-linear and the coefficients cannot be measured, making accurate orthogonal steering very challenging. Moreover, the presence of a quadrupole between MCAWA.412347 and MCAWA.412349 acted as a further source of errors (wrong calibration, fringe fields, field non-linearities). To address this issue and to reduce at the same time the beam free propagation distance after the last steering element, a new corrector, MCAWA.412353, was installed on the beam line. In the new configuration, no active elements are present between correctors and the matrix elements depend only on the drift lengths and are equal in the x and y plane. This limits the source of errors and reduces the number of kick-response scans needed to measure the response matrix coefficients (2 instead of 4).

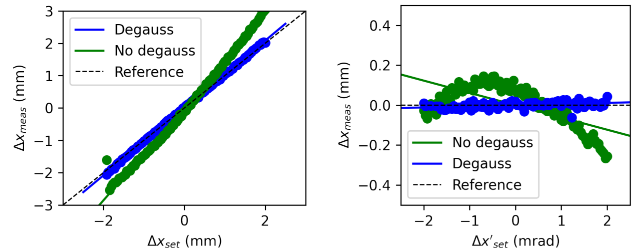

(a) Scan Δx, $\Delta x' = 0$ (b) Scan $\Delta x'$, $\Delta x = 0$

Figure 2: Measured response at BTV.412354 to orthogonal steering with and without quick demagnetisation cycle.

Hysteresis effects can be mitigated by performing demagnetisation cycles. However, a complete cycle is time-consuming (a few minutes). Since orthogonal steering is used to perform angular and position scans, adding a downtime of few minutes at every step of the scan would result in an unacceptable downtime.

The reproducibility issue was addressed by adding a simplified version of the demagnetisation cycle before setting any new corrector current. The current is set to its minimum current, its maximum current and at last to the setting point. Several tests were performed to assess the effectiveness of this approach, which revealed very good reproducibility. The limitation of this approach is that the response matrix does not match the theoretical one and must, therefore, be measured. The scan takes a few minutes and should be performed once a day, after the RF gun is switched on and the operational parameters are optimised.

The method and the whole workflow were tested at the beginning of 2023, after the new corrector (MCAWA.412353) was installed. The observation point was BTV.412354 instead of the BTV.EXP_VOL, since the latter was temporarily removed from the beam line. To perform the test, the response coefficients $R_{1,(1,2)}$ and $R_{2,(1,2)}$ were measured ($R_{1,(2,2)}$ and $R_{1,(2,2)}$ are equal to 1) and plugged into the script developed to perform orthogonal steering. To assess the robustness of the method, two scans were performed. A position scan (Δx) with parallel beam ($\Delta x' = 0$) and an angular (Δx) scan keeping the beam stable on the same point (($\Delta x = 0$)). The range for the test was chosen to be (−2 mm,2 mm) for the position and (−2 mrad, 2 mrad) for the angle, which is more than sufficient for the purposes of the experiment.

The results of the measurements (Fig. 2a and Fig. 2b) show that, with the demagnetisation procedure, the measured and setting points match very well and the hysteresis effects are fully compensated. The new method will be included as standard operational procedure during 2023 run.

ONLINE BEAM SIZE OPTIMISATION

The parameters of the laser and the S-band accelerating cavities are tuned every morning to find the best operational configuration. This procedure results in slight change in beam parameters at the entrance of the beam line and hence

ISBN: 978-3-95450-231-8 ISSN: 2673-5490 doi: 10.18429/JACoW-IPAC2023-MOPA103

in a change of the beam distribution at the entrance of the plasma source. To quickly rematch the beam line, a numerical optimisation approach was developed and tested, starting from the results reported in [9]. For the 2022 run, a few changes were made to tailor the algorithm to the new experimental requirements.

The algorithm changes the field strength in the first three quadrupoles of the line and optimises an objective function f_{obj} built on the image observed at BTV.EXP_VOL. In particular the objective function is defined as follows:

$$f_{obj} = w_1(\sigma_{x,m} - \sigma_{x,t}) + w_2(\sigma_{y,m} - \sigma_{y,t}) \\ +w_3(|\sigma_x - \sigma_y|) + w_4 KL_{div}$$

where $\sigma_{x,m}$,$\sigma_{y,m}$ are the measured beam size in x and y, $\sigma_{x,t}$,$\sigma_{y,t}$ are target beam sizes ($\sigma_{x,t}$,$\sigma_{y,t}$=200 µm) and KL_{div} is the Kullback-Leibler divergence [10] between the measured data and a Gaussian distribution fitted on the same data (this last term allows to improve the distribution of the beam delivered to the plasma cell). $w_{1,\ldots,4}$ are the weights per term of the loss function. The Powell algorithm Bound Optimization BY Quadratic Approximation (BOBYQA) was chosen, as implemented in Ref. [11]. This algorithm is very effective when function evaluations are expensive and where the objective function is noisy [9]. An example of the outcome of the optimisation is shown in Fig. 3.

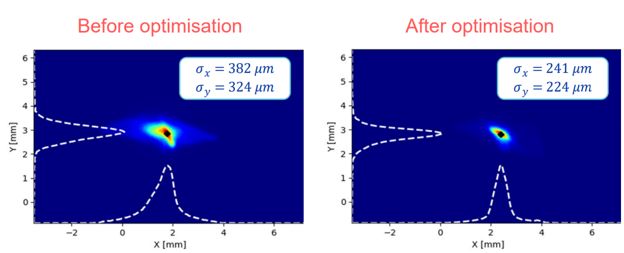

Figure 3: Beam distribution measured at BTV.EXP_VOL before and after optimisation.

EMITTANCE RECONSTRUCTION

The default method for measuring the emittance at the entrance of the beam line is based on the quadrupole scan technique [8]. For each quadrupole setting, the beam size is calculated from a Gaussian fit on the x and y projections, which are extrapolated from the image recorded at BTV.412342. As explained in [8], by fitting a parabolic function to the square of the beam sizes, it is possible to calculate the Twiss parameters at the entrance of the quadrupole. The technique is very effective when dealing with Gaussian distributions, but it loses accuracy as the distribution differs from a Gaussian.

To deal with non-Gaussian beams, phase space tomographic techniques can be used. The physics of a beam transported in a quadrupole-drift section can be described by a transport matrix $M(k)$, where k is the quadrupole strength. The transport can be seen as a combination of a rotation

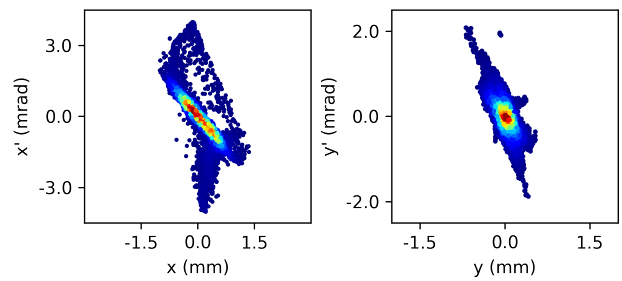

(a)

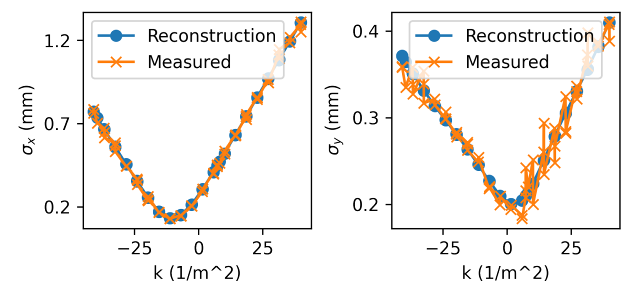

(b)

Figure 4: Reconstructed distribution (a) in $x - x'$ and $y - y'$ respectively. In (b) a comparison between the measured and the reconstructed beam sizes in the x (left) and y (right) plane respectively.

and a sheer, and applying the appropriate manipulations, the quadrupole scan can be approached as a classical tomography problem [12], and the same algorithms can be used. For this work, the Maximum Likelihood Maximum Expectation (MLEM) algorithm was used [13]. MLEM is particularly suited when a limited range of projections is available. The method was developed and commissioned using different simulated beams, and then validated with data.

The result of the reconstruction applied to a quadrupole scan taken on the beam line is shown in Fig. 4. Fig. 4a shows the reconstructed distribution at the entrance of the quadrupole used for the scan, while Fig. 4b shows how the reconstructed beam sizes (obtained by simulating the quadrupole scan with the reconstructed distribution) compare with the measured ones. It can be clearly seen that the reconstruction allows to reproduce the non-linear features of the beam and to reproduce the measured beam sizes at the BTV.

CONCLUSIONS

A set of new operational tools were developed during 2022 to address the new, tighter experimental requirements needed to perform hosing studies at AWAKE. In particular, a method to efficiently perform orthogonal steering in a reproducible way was developed, together with an online beam size optimiser and a tool for phase space tomography. All the tools were successfully tested and will allow for a better characterization of the beam line and more reproducible and flexible operation during Run2b.

Content from this work may be used under the terms of the CC BY 4.0 licence (© 2022). Any distribution of this work must maintain attribution to the author(s), title of the work, publisher, and DOI.

ISBN: 978-3-95450-231-8 ISSN: 2673-5490 doi: 10.18429/JACoW-IPAC2023-MOPA103

Content from this work may be used under the terms of the CC BY 4.0 licence (© 2022). Any distribution of this work must maintain attribution to the author(s), title of the work, publisher, and DOI.

REFERENCES

[1] E. Adli, *et al.* (AWAKE Collaboration), "Acceleration of electrons in the plasma wakefield of a proton bunch," *Nature*, vol. 561, no. 7723, pp. 363–367, 2018. DOI: 10.1038/s41586-018-0485-4.

[2] P. Muggli for the AWAKE Collaboration, "Physics to plan AWAKE Run 2," in *Journal of Physics: Conference Series*, IOP Publishing, vol. 1596, 2020, p. 012 008. DOI: 10.1088/1742-6596/1596/1/012008.

[3] L. Verra, *et al.* (AWAKE Collaboration), "Controlled growth of the self-modulation of a relativistic proton bunch in plasma," *Phys. Rev. Lett.*, vol. 129, no. 2, p. 024 802, 2022. DOI: 10.1103/PhysRevLett.129.024802.

[4] T. Nechaeva and P. Muggli, "Hosing of a long proton bunch induced by an electron bunch," in *Proc. 48th EPS Conference on Plasma Physics*, 2022.

[5] C. Bracco *et al.*, "Systematic Optics Studies for the Commissioning of the AWAKE Beamline," in *Proc. IPAC'19*, (Melbourne, Australia, May 2019), JACoW Publishing, Geneva, Switzerland, pp. 2383–2386. DOI: 10.18429/JACoW-IPAC2019-WEPMP029. http://accelconf.web.cern.ch/ipac2019/papers/WEPMP029.pdf

[6] S.-Y. Kim *et al.*, "Commissioning of the electron injector for the AWAKE experiment," *Nucl. Instrum. Meth. A*, vol. 953, p. 163 194, 2020. DOI: 10.1016/j.nima.2019.163194.

[7] J. S. Schmidt *et al.*, "The AWAKE Electron Primary Beam Line," in *Proc. IPAC'15*, (Richmond, VA, USA, May 2015), JACoW Publishing, Geneva, Switzerland, pp. 2584–2586. DOI: 10.18429/JACoW-IPAC2015-WEPWA039. https://jacow.org/IPAC2015/papers/WEPWA039.pdf

[8] M. Minty, "Diagnostics ii," *CERN Accelerator School, Sept. 2004.*, 2004.

[9] F. M. Velotti, B. Goddard, V. Kain, R. Ramjiawan, G. Zevi Della Porta, and S. Hirlaender, "Towards automatic setup of 18 mev electron beamline using machine learning," *Machine Learning: Science and Technology*, 2023. DOI: 10.1088/2632-2153/acce21.

[10] S. Kullback and R. A. Leibler, "On information and sufficiency," *The annals of mathematical statistics*, vol. 22, no. 1, pp. 79–86, 1951. DOI: 10.1214/aoms/1177729694.

[11] *Py-BOBYQA: Derivative-Free Solver for Bound-Constrained Minimization*, https://github.com/numericalalgorithmsgroup/pybobyqa, 2021.

[12] K. Hock and A. Wolski, "Tomographic reconstruction of the full 4d transverse phase space," *Nuclear Instruments and Methods in Physics Research Section A: Accelerators, Spectrometers, Detectors and Associated Equipment*, vol. 726, pp. 8–16, 2013. DOI: 10.1016/j.nima.2013.05.004.

[13] L. Sheep, "Maximum likelihood reconstruction for emission tomography," *IEEE Trans Med Imaging*, pp. 112–113, 1982. DOI: 10.1109/TMI.1982.4307558.